Exploring neutrino mass and mass hierarchy in the scenario of vacuum energy interacting with cold dark matter [*]

Rui-Yun Guo(郭瑞芸)[1]   Jing-Fei Zhang(张敬飞)[1]   Xin Zhang(张鑫)[1,2;1]

[1] Department of Physics, College of Sciences, Northeastern University, Shenyang 110819, China
[2] Center for High Energy Physics, Peking University, Beijing 100080, China

Abstract: We investigate the constraints on total neutrino mass in the scenario of vacuum energy interacting with cold dark matter. We focus on two typical interaction forms, i.e., $Q=\beta H\rho_{\rm c}$ and $Q=\beta H\rho_{\Lambda}$. To avoid the occurrence of large-scale instability in interacting dark energy cosmology, we adopt the parameterized post-Friedmann approach to calculate the perturbation evolution of dark energy. We employ observational data, including the Planck cosmic microwave background temperature and polarization data, baryon acoustic oscillation data, a JLA sample of type Ia supernovae observation, direct measurement of the Hubble constant, and redshift space distortion data. We find that, compared with those in the ΛCDM model, much looser constraints on $\sum m_{\nu}$ are obtained in the $Q=\beta H\rho_{\rm c}$ model, whereas slightly tighter constraints are obtained in the $Q=\beta H\rho_{\Lambda}$ model. Consideration of the possible mass hierarchies of neutrinos reveals that the smallest upper limit of $\sum m_{\nu}$ appears in the degenerate hierarchy case. By comparing the values of $\chi^2_{\rm min}$, we find that the normal hierarchy case is favored over the inverted one. In particular, we find that the difference $\Delta\chi^2_{\rm min}\equiv\chi^2_{\rm IH;min}-\chi^2_{\rm NH;min}>2$ in the $Q=\beta H\rho_{\rm c}$ model. In addition, we find that $\beta=0$ is consistent with the current observations in the $Q=\beta H\rho_{\rm c}$ model, and $\beta<0$ is favored at more than the 1σ level in the $Q=\beta H\rho_{\Lambda}$ model.

Keywords: interacting dark energy, neutrino mass, mass hierarchy of neutrinos, parameterized post-Friedmann approach, cosmological observations

PACS: 95.36.+x, 98.80.Es, 98.80.-k   **DOI:** 10.1088/1674-1137/42/9/095103

1   Introduction

The phenomenon of neutrino oscillation has proved that neutrinos have masses and that there are mass splittings between different neutrino species (see Refs. [1, 2] for reviews). However, it is enormously difficult for particle physics experiments to directly measure the absolute masses of neutrinos. In fact, the solar and reactor experiments measured the squared mass difference, $\Delta m^2_{21}\simeq7.5\times10^{-5}$ eV^2, and the atmospheric and accelerator beam experiments measured the squared mass difference, $|\Delta m^2_{31}|\simeq2.5\times10^{-3}$ eV^2 [2]. Thus, two possible mass hierarchies are obtained, i.e., the normal hierarchy (NH) with $m_1<m_2\ll m_3$ and the inverted hierarchy (IH) with $m_3\ll m_1<m_2$, where m_i ($i=1$, 2, 3) denotes the masses of neutrinos in the three mass eigenstates. If the mass splittings are neglected, we then have $m_1=m_2=m_3$, which represents the degenerate hierarchy (DH).

Actually, the absolute masses of neutrinos could in principle be measured by particle physics experiments, such as tritium beta decay experiments [3–6] and neu-

trinoless double beta decay ($0\nu\beta\beta$) experiments [7, 8]. In addition, experiments for detecting cosmic relic neutrinos (e.g., the PTOLEMY proposal [9–12]) are also able to measure the absolute masses of neutrinos. However, compared with these particle physics experiments, cosmological observations are considered to be a more promising method to determine the absolute masses of neutrinos. Massive neutrinos can leave rich signatures on the cosmic microwave background (CMB) anisotropies and the large-scale structure (LSS) formation in the evolution of the universe. Thus, one might extract useful information on neutrinos from these available cosmological observations.

Recently, the constraint on the total neutrino mass has been reduced to $\sum m_{\nu}<0.15$ eV (2σ) [13] in the base Λ cold dark matter (ΛCDM) model. For dynamical dark energy models, the constraints become $\sum m_{\nu}<0.25$ eV (2σ) in the wCDM model and $\sum m_{\nu}<0.51$ eV (2σ) in the Chevallier–Polarski–Linder (CPL) model [13], indicating that larger neutrino masses are favored in the two dynamical dark energy models. However, in the holo-

graphic dark energy (HDE) model, the constraint result is reduced to $\sum m_\nu < 0.113$ eV (2σ) [14], which is close to the edge of diagnosing the mass hierarchy of neutrinos. For more studies on constraining the total neutrino mass in cosmological models, see, e.g., Refs. [15–46].

Furthermore, when the possible mass hierarchies of neutrinos are considered, some previous studies showed that the NH case fits cosmological observations better than the IH case. For example, Huang et al. [47] gave the result $\Delta\chi^2 \equiv \chi^2_{\rm IH;min} - \chi^2_{\rm NH;min} \simeq 3.38$ in the ΛCDM model; Wang et al. [48] gave the results $\Delta\chi^2 \simeq 2.1$ in the wCDM model and $\Delta\chi^2 \simeq 4.1$ in the HDE model. Further, when the DH case is included for comparison, the DH case fits almost all of the data combinations best. Consistent conclusions are also obtained in the CPL model [49].

In addition, when interaction between dark energy and dark matter is considered in current cosmology, the constraint on $\sum m_\nu$ is reduced to $\sum m_\nu < 0.10$ eV (2σ) [50]. This result implies that the IH case in this scenario should be excluded by current observations. Actually, however, the small upper limit obtained is due mainly to the strong tension between the Planck data and the latest Hubble constant measurement. Moreover, in the study in Ref. [50], the possible mass hierarchies of neutrinos are not considered. Thus, in the present work, we will revisit the constraints on the total neutrino mass in the interacting dark energy (IDE) scenario, and the mass hierarchy cases of neutrinos will be considered for the first time in this scenario.

The IDE scenario refers to a cosmological model in which direct exchanges of energy and momentum between dark energy and dark matter are considered. This scheme has been proposed and studied widely in the literature [51–92]. The cosmic coincidence problem can be greatly alleviated in this situation [53–55, 64, 66]. Searching for interactions between dark energy and dark matter observationally is an important mission in cosmology. The impacts of interactions between dark energy and dark matter on the CMB [66, 84] and LSS [52, 60, 64, 67, 78, 84] have been investigated in detail.

In our work, we investigate a specific class of models of IDE, in which dark energy is considered to be the vacuum energy with $w = -1$, and thus the interaction is between vacuum energy and cold dark matter. In the usual ΛCDM model, the vacuum energy density is equivalent to the cosmological constant Λ, and in this case, the vacuum energy is a pure background with a constant Λ. However, when the interaction is considered, the vacuum energy density is no longer a constant, and thus it is no longer a pure background. A model with such a setting is sometimes called the $\Lambda(t)$CDM model. In this paper, in order to be consistent with our previous studies, we call these models IΛCDM models.

The energy conservation equations of the vacuum energy density (ρ_Λ) and the cold dark matter density ($\rho_{\rm c}$) in this scenario are given by

$$\dot{\rho}_\Lambda = Q, \tag{1}$$

$$\dot{\rho}_{\rm c} = -3H\rho_{\rm c} - Q, \tag{2}$$

where a dot represents the derivative with respect to the cosmic time t, H is the Hubble parameter, and Q is the energy transfer rate. In this work, we employ two phenomenological forms of Q, i.e., $Q = \beta H \rho_{\rm c}$ and $Q = \beta H \rho_\Lambda$, where β represents a dimensionless coupling parameter. From Eqs. (1) and (2), it can be seen that $\beta > 0$ indicates that the energy transport is from dark matter to vacuum energy, $\beta < 0$ represents an inverse energy flow, and $\beta = 0$ indicates no interaction between vacuum energy and cold dark matter.

Here we note that the above IΛCDM models are based on purely phenomenological considerations. Because we do not understand the microscopic mechanism of how dark matter feels a "fifth force" through the mediation of dark energy, we cannot describe this process by a Lagrangian. In fact, we cannot write Lagrangians for most uncoupled dark energy models, let alone for IDE models. Only for some very specific dark energy models, e.g., the "quintessence" scalar field model, is a Lagrangian description possible. For the coupled quintessence model, the Lagrangian in the Einstein frame is given by $\mathcal{L} = -\frac{1}{2}\partial^\mu \phi \partial_\mu \phi - V(\phi) - m(\phi)\overline{\psi}\psi + \mathcal{L}_{\rm kin}[\psi]$, where $m(\phi)$ is the mass of the dark matter field ψ, which is a function of the quintessence scalar field ϕ in this scenario. Actually, in this scenario, the forms of the quintessence potential $V(\phi)$ and the dark matter mass $m(\phi)$ also need to be assumed. To investigate the interaction between dark energy and dark matter, it is usually better to consider more phenomenological scenarios (just as in the study of dynamical dark energy, some parametrization models are more apt to be linked to actual observations). In such a description, an analogy with the reheating process in the inflationary cosmology or the nuclear decay process is often made. Namely, one assumes the form of the energy transfer rate and then writes the energy continuity equations for dark energy and dark matter. For the IΛCDM models studied in this paper, we actually do not consider the fundamental theory behind them, but we adopt only a purely phenomenological perspective. In this scenario, the number of parameters is the same as that in the wCDM cosmology. However, here we also note that the scenario of a "running" vacuum energy density can actually be related to the renormalization group; see, e.g., Refs. [82, 86, 90, 92].

Recently, some exciting studies [50, 82, 86, 90, 92–94] found a nonzero interaction between dark sectors at more than the 1σ level. For example, Salvatelli et al. [93] showed that a nonzero interaction is favored at late times. In their work, ten data points from redshift space

distortion (RSD) measurements can break the degeneracy between $\Omega_c h^2$ and β. This can impose a lower limit on $\Omega_c h^2$ and lead to a shift of β. Actually, when only the RSD data from DR12 are included, $\beta = 0$ is still favored by current observational data. In addition, in Refs. [50, 94], β is positively correlated with $\sum m_\nu$ in the $Q = \beta H \rho_c$ model. A larger neutrino mass is derived in this scenario than in the ΛCDM model. Thus, a positive value of β is favored at more than the 1σ level. From the above analysis, we conclude that a nonzero interaction is always dependent on observational data or the model itself.

In this paper, we report the latest results of constraints on the total neutrino mass in the IΛCDM models. For the neutrino mass measurement, we consider the NH case, the IH case, and the DH case. Some important questions will be addressed in this work: (i) Compared with those in the ΛCDM model, what upper bounds of $\sum m_\nu$ will be obtained in the IΛCDM models? (ii) Which hierarchy of neutrino masses will be favored in the IΛCDM models? (iii) Can a nonzero interaction be detected by current cosmological observations?

The structure of the paper is as follows. In Section **2**, we first introduce the observational data employed in this paper, and then we describe the constraint method used in our analysis. In Section **3**, we analyze the results of constraining the coupling constant and the neutrino mass in the IΛCDM scenario. The issue of diagnosing the neutrino mass hierarchy will also be discussed in this section. Finally, we give the conclusions of the entire work in Section **4**.

2   Data and method

In what follows, we briefly describe the observational data used in this work. They are:

1) Planck TT, TE, EE + lowP: We employ the likelihood, including the TT, EE, and TE spectra, as well as the Planck low-ℓ ($\ell \leq 30$) likelihood, from the Planck 2015 release [30].

2) BAO: We consider the four baryon acoustic oscillation (BAO) data points, that is, the SDSS-MGS measurement at $z_{\mathrm{eff}} = 0.15$ [95], the 6dFGS measurement at $z_{\mathrm{eff}} = 0.106$ [96], and the CMASS and LOWZ samples from the BOSS DR12 at $z_{\mathrm{eff}} = 0.57$ and $z_{\mathrm{eff}} = 0.32$ [97].

3) SNIa: We employ the Joint Light-curve Analysis (JLA) compilation of type Ia supernovae [98]. It contains 740 type Ia supernovae data obtained from SNLS and SDSS as well as a few samples of low-redshift light-curve analysis.

4) H_0: We use the new result of direct measurement of the Hubble constant, $H_0 = 73.00 \pm 1.75$ km s^{-1} Mpc^{-1} [99]. It reduced the uncertainty from 3.3% to 2.4% by using Wide Field Camera 3 on the Hubble Space Telescope. However, there is a strong tension between the new H_0 measurement and the Planck data. This reminds us to use these data in an appropriate way.

5) RSD: We employ two RSD data points obtained from the LOWZ sample at $z_{\mathrm{eff}} = 0.32$ and the CMASS sample at $z_{\mathrm{eff}} = 0.57$ of the BOSS DR12 [100]. Because these two RSD data points also include the corresponding BAO measurements, we exclude the BAO measurements of Ref. [97] from the BAO likelihood in the combined constraints applied in this paper to avoid double counting.

We consider two data combinations in this work, i.e., Planck TT, TE, EE + lowP + BAO + SNIa + RSD and Planck TT, TE, EE + lowP + BAO + SNIa + RSD + H_0. It should be pointed out that when the latest local measurement of H_0 is included in an analysis, an additional parameter N_{eff} considered in the cosmological models will be more helpful for relieving the tension [24, 26, 99, 101–105].

Actually, there are also other measurements of the growth of structure that are often used to constrain the total neutrino mass, for example, the CMB lensing, galaxy weak lensing, and cluster counts measurements. In this paper, we consider only the above two data combinations, mainly because they are convenient for making a direct comparison with the results of Ref. [50]. In addition, the consistency with the Planck CMB power spectra is also taken into account. In fact, it is expected that inclusion of the Planck lensing likelihood would lead to somewhat weaker constraints on the neutrino mass owing to the low values of σ_8 preferred by Planck lensing. Galaxy weak lensing probes lower redshifts and smaller spatial scales than CMB lensing, and thus the uncertainties in modeling nonlinearities in the matter power spectrum and the baryonic feedback on these scales become rather important. To mitigate the uncertainties of the nonlinear modeling, a conservative cut scheme can be adopted for the weak lensing data [106], but this treatment would greatly weaken the constraining power of the weak lensing data. Moreover, both galaxy weak lensing and cluster counts actually remain in tension with the Planck CMB data, even though massive neutrinos are considered in a cosmological model [30]. Therefore, these measurements of structural growth are not used in this paper.

In the IΛCDM cosmology, we must consider the large-scale instability problem [63] seriously. To resolve this problem, we adopt the parameterized post-Friedmann (PPF) approach [50, 107–110]. It is an effective scheme to treat the perturbations of dark energy. On large scales, a direct relationship is established between the velocities of dark energy and other components. On small scales, the Poisson equation can effectively describe curvature perturbations. In order to be consistent on all

scales, a dynamical function Γ is constructed to link them. By combining the Einstein equations with the conservation equations, the equation of motion of Γ can be determined. Then we can obtain the correct energy density and velocity perturbations of dark energy. This PPF scheme can help us explore the entire parameter space of the IΛCDM models without assuming any specific ranges of w and β.

For the base ΛCDM model, the six basic cosmological parameters are $\{\omega_{\rm b}, \omega_{\rm c}, \theta_{\rm MC}, \tau, n_{\rm s}, \ln(10^{10}A_{\rm s})\}$. Here $\omega_{\rm b}=\Omega_{\rm b}h^2$ is the present density of baryons, and $\omega_{\rm c}=\Omega_{\rm c}h^2$ is the present density of cold dark matter; $\theta_{\rm MC}$ is the ratio between the sound horizon and the angular diameter distance at the decoupling epoch; τ is the Thomson scattering optical depth resulting from reionization; $n_{\rm s}$ is the scalar spectral index; and $A_{\rm s}$ is the amplitude of the primordial power spectrum at the pivot scale, $k_p = 0.05$ Mpc^{-1}. For the IΛCDM models, the prior range of the coupling parameter β is set to $[-0.2, 0.2]$ for the case of $Q=\beta H\rho_{\rm c}$ and $[-1.0, 1.0]$ for the case of $Q=\beta H\rho_{\Lambda}$. The additional free parameters include the total neutrino mass $\sum m_\nu$ and the effective number of relativistic species, $N_{\rm eff}$, with a prior of $[0, 6.0]$.

To constrain the neutrino mass and other cosmological parameters, we employ a modified version of the publicly available CosmoMC sampler [111]. The posterior distributions of all the cosmological parameters can be obtained by fitting to observational data.

For the NH case, the neutrino mass spectrum is

$$(m_1, m_2, m_3) = (m_1, \sqrt{m_1^2 + \Delta m_{21}^2}, \sqrt{m_1^2 + |\Delta m_{31}^2|}) \quad (3)$$

in terms of a free parameter m_1. For the IH case, the neutrino mass spectrum is

$$(m_1, m_2, m_3) = (\sqrt{m_3^2 + |\Delta m_{31}^2|}, \sqrt{m_3^2 + |\Delta m_{31}^2| + \Delta m_{21}^2}, m_3) \quad (4)$$

in terms of a free parameter m_3. We also consider the DH case for comparison. In this case, the neutrino mass spectrum is

$$m_1 = m_2 = m_3 = m, \quad (5)$$

where m is a free parameter. It should be pointed out that the input lower bounds of $\sum m_\nu$ are 0.06 eV for the NH case, 0.10 eV for the IH case, and 0 eV for the DH case.

3   Results

We constrain the total neutrino mass in the IΛCDM models. For comparison with Ref. [50], we further consider the three mass hierarchy cases of neutrinos, i.e., the NH case, the IH case, and the DH case. Our fitting results are listed in Tables 1 and 2 for the base ΛCDM model and Tables 3–6 for the two IΛCDM models. For convenient display, we use "IΛCDM1" and "IΛCDM2"

instead of "the $Q\propto\rho_{\rm c}$ model" and "the $Q\propto\rho_{\Lambda}$ model," respectively. In these tables, we quote the $\pm1\sigma$ errors of cosmological parameters, but only the 2σ upper limit is given for the total neutrino mass $\sum m_\nu$. In addition, we also list the values of $\chi^2_{\rm min}$.

3.1   Neutrino mass

We first use the Planck TT, TE, EE + lowP + BAO + SNIa + RSD data combination to constrain these models. In the ΛCDM+$\sum m_\nu$ model, we obtain $\sum m_\nu < 0.217$ eV for the NH case, $\sum m_\nu < 0.235$ eV for the IH case, and $\sum m_\nu < 0.198$ eV for the DH case (see Table 1). In the IΛCDM1+$\sum m_\nu$ model, the constraint results become $\sum m_\nu < 0.279$ eV for the NH case, $\sum m_\nu < 0.301$ eV for the IH case, and $\sum m_\nu < 0.245$ eV for the DH case (see Table 3), indicating that much looser constraints are obtained than those in the ΛCDM+$\sum m_\nu$ model. Further, in the IΛCDM2+$\sum m_\nu$ model, the results are $\sum m_\nu < 0.206$ eV for the NH case, $\sum m_\nu < 0.228$ eV for the IH case, and $\sum m_\nu < 0.180$ eV for the DH case (see Table 5), indicating that the constraints are slightly tighter than those in the ΛCDM+$\sum m_\nu$ model.

Furthermore, we consider including the latest local measurement of the Hubble constant, $H_0 = 73.00 \pm 1.75$ km s^{-1} Mpc^{-1}, to constrain these models. Using the Planck TT, TE, EE + lowP + BAO + SNIa + RSD + H_0 data combination, we find that, compared with the ΛCDM+$\sum m_\nu$+$N_{\rm eff}$ model, the IΛCDM1+$\sum m_\nu$+$N_{\rm eff}$ model provides much looser constraints on $\sum m_\nu$, whereas the IΛCDM2+$\sum m_\nu$+$N_{\rm eff}$ model provides tighter constraints. This is consistent with the case using the Planck TT, TE, EE + lowP + BAO + SNIa + RSD data. The detailed results are given in Tables 2, 4, and 6. Considering the three mass hierarchies, we find that the value of $\sum m_\nu$ is smallest in the DH case and largest in the IH case. Thus, the mass hierarchy can affect the constrained values of $\sum m_\nu$ in these models.

Next, we give the values of $\chi^2_{\rm min}$ for the three mass hierarchy cases. For the ΛCDM+$\sum m_\nu$ model and the ΛCDM+$\sum m_\nu$+$N_{\rm eff}$ model, we find that the values of $\chi^2_{\rm min}$ in the NH case are slightly smaller than those in the IH case, and the difference $\Delta\chi^2_{\rm min} \equiv \chi^2_{\rm IH;min} - \chi^2_{\rm NH;min} < 2$ (see Tables 1 and 2). When the mass splittings are neglected, the values of $\chi^2_{\rm min}$ are smallest in this case. In addition, for the IΛCDM1+$\sum m_\nu$ model and the IΛCDM1+$\sum m_\nu$+$N_{\rm eff}$ model, we find that the difference $\Delta\chi^2_{\rm min} \equiv \chi^2_{\rm IH;min} - \chi^2_{\rm NH;min} > 2$ (see Tables 3 and 4), further providing strong support for the NH case. In this situation, the values of $\chi^2_{\rm min}$ for the DH case are the smallest. For the IΛCDM2+$\sum m_\nu$ model and the IΛCDM2+$\sum m_\nu$+$N_{\rm eff}$ model, we obtain results consistent with those in the ΛCDM+$\sum m_\nu$ model and the ΛCDM+$\sum m_\nu$+$N_{\rm eff}$ model. Namely, the NH case is

Table 1.   Fitting results of the cosmological parameters in the ΛCDM+$\sum m_\nu$ model for mass hierarchy cases NH, IH, and DH.

data	Planck TT,TE,EE+lowP+BAO+SNIa+RSD		
model	ΛCDM+$\sum m_\nu^{\mathrm{NH}}$	ΛCDM+$\sum m_\nu^{\mathrm{IH}}$	ΛCDM+$\sum m_\nu^{\mathrm{DH}}$
$\Omega_b h^2$	0.02231 ± 0.00014	0.02232 ± 0.00014	0.02230 ± 0.00014
$\Omega_c h^2$	0.1186 ± 0.0011	0.1183 ± 0.0011	0.1188 ± 0.0012
$100\theta_{\mathrm{MC}}$	1.04087 ± 0.00029	1.04087 ± 0.00030	1.04084 ± 0.00029
τ	$0.078^{+0.017}_{-0.016}$	$0.082^{+0.017}_{-0.016}$	0.074 ± 0.017
$\ln(10^{10}A_s)$	3.087 ± 0.032	3.094 ± 0.032	3.080 ± 0.033
n_s	0.9672 ± 0.0042	0.9678 ± 0.0041	0.9665 ± 0.0042
$\sum m_\nu$	<0.217 eV	<0.235 eV	<0.198 eV
Ω_{m}	$0.3139^{+0.0071}_{-0.0072}$	$0.3159^{+0.0069}_{-0.0070}$	$0.3116^{+0.0072}_{-0.0081}$
H_0	$67.31^{+0.59}_{-0.54}$	$67.13^{+0.53}_{-0.52}$	$67.53^{+0.64}_{-0.57}$
χ^2_{min}	13661.472	13661.662	13658.622

Table 2.   Fitting results of the cosmological parameters in the ΛCDM+$\sum m_\nu$+N_{eff} model for mass hierarchy cases NH, IH, and DH.

data	Planck TT,TE,EE+lowP+BAO+SNIa+RSD+H_0		
model	ΛCDM+$\sum m_\nu^{\mathrm{NH}}$+N_{eff}	ΛCDM+$\sum m_\nu^{\mathrm{IH}}$+N_{eff}	ΛCDM+$\sum m_\nu^{\mathrm{DH}}$+N_{eff}
$\Omega_b h^2$	$0.02252^{+0.00017}_{-0.00018}$	0.02256 ± 0.00017	0.02248 ± 0.00018
$\Omega_c h^2$	0.1214 ± 0.0028	0.1217 ± 0.0027	$0.1211^{+0.0027}_{-0.0028}$
$100\theta_{\mathrm{MC}}$	1.04058 ± 0.00041	1.04054 ± 0.00040	1.04063 ± 0.00040
τ	0.082 ± 0.017	0.086 ± 0.017	0.077 ± 0.017
$\ln(10^{10}A_s)$	3.103 ± 0.034	3.112 ± 0.034	3.093 ± 0.035
n_s	$0.9761^{+0.0067}_{-0.0068}$	$0.9778^{+0.0066}_{-0.0067}$	$0.9740^{+0.0068}_{-0.0073}$
$\sum m_\nu$	<0.227 eV	<0.249 eV	<0.202 eV
N_{eff}	3.27 ± 0.16	3.30 ± 0.16	3.23 ± 0.16
Ω_{m}	$0.3058^{+0.0068}_{-0.0067}$	0.3071 ± 0.0067	$0.3040^{+0.0069}_{-0.0068}$
H_0	68.93 ± 0.97	68.94 ± 0.97	68.94 ± 0.98
χ^2_{min}	13669.956	13670.988	13668.192

Table 3.   Fitting results of the cosmological parameters in the IΛCDM1 ($Q=\beta H\rho_{\mathrm{c}}$)+$\sum m_\nu$ model for mass hierarchy cases NH, IH, and DH.

data	Planck TT,TE,EE+lowP+BAO+SNIa+RSD		
model	IΛCDM1+$\sum m_\nu^{\mathrm{NH}}$	IΛCDM1+$\sum m_\nu^{\mathrm{IH}}$	IΛCDM1+$\sum m_\nu^{\mathrm{DH}}$
$\Omega_b h^2$	0.02228 ± 0.00015	0.02227 ± 0.00016	0.02229 ± 0.00015
$\Omega_c h^2$	$0.1182^{+0.0014}_{-0.0013}$	$0.1178^{+0.0015}_{-0.0013}$	$0.1187^{+0.0015}_{-0.0013}$
$100\theta_{\mathrm{MC}}$	1.04087 ± 0.00030	1.04088 ± 0.00030	1.04085 ± 0.00030
τ	0.078 ± 0.017	0.081 ± 0.017	0.074 ± 0.017
$\ln(10^{10}A_s)$	3.089 ± 0.033	$3.095^{+0.033}_{-0.032}$	3.081 ± 0.033
n_s	0.9667 ± 0.0043	0.9669 ± 0.0044	0.9663 ± 0.0044
β	0.0010 ± 0.0018	$0.0014^{+0.0017}_{-0.0018}$	0.0004 ± 0.0018
$\sum m_\nu$	<0.279 eV	<0.301 eV	<0.245 eV
Ω_{m}	0.3116 ± 0.0090	0.3121 ± 0.0090	$0.3112^{+0.0090}_{-0.0089}$
H_0	67.52 ± 0.74	67.47 ± 0.74	$67.57^{+0.73}_{-0.74}$
χ^2_{min}	13660.994	13663.684	13661.990

Table 4.   Fitting results of the cosmological parameters in the IΛCDM1 $(Q=\beta H\rho_c)+\sum m_\nu+N_{\rm eff}$ model for mass hierarchy cases NH, IH, and DH.

data	Planck TT,TE,EE+lowP+BAO+SNIa+RSD+H_0		
model	IΛCDM1+$\sum m_\nu^{\rm NH}$+$N_{\rm eff}$	IΛCDM1+$\sum m_\nu^{\rm IH}$+$N_{\rm eff}$	IΛCDM1+$\sum m_\nu^{\rm DH}$+$N_{\rm eff}$
$\Omega_b h^2$	0.02244 ± 0.00021	0.02244 ± 0.00021	0.02242 ± 0.00021
$\Omega_c h^2$	0.1201 ± 0.0032	0.1200 ± 0.0032	0.1203 ± 0.0032
$100\theta_{\rm MC}$	1.04067 ± 0.00042	1.04064 ± 0.00042	1.04068 ± 0.00042
τ	$0.081^{+0.018}_{-0.017}$	0.084 ± 0.018	0.077 ± 0.017
$\ln(10^{10}A_s)$	$3.102^{+0.036}_{-0.035}$	$3.109^{+0.036}_{-0.035}$	3.093 ± 0.035
n_s	0.9738 ± 0.0078	$0.9744^{+0.0078}_{-0.0077}$	$0.9724^{+0.0078}_{-0.0077}$
β	0.0015 ± 0.0019	0.0018 ± 0.0019	$0.0010^{+0.0019}_{-0.0021}$
$\sum m_\nu$	<0.296 eV	<0.321 eV	<0.263 eV
$N_{\rm eff}$	3.22 ± 0.18	3.23 ± 0.17	3.20 ± 0.17
$\Omega_{\rm m}$	$0.3024^{+0.0081}_{-0.0080}$	0.3029 ± 0.0082	0.3021 ± 0.0082
H_0	$69.05^{+0.99}_{-0.98}$	69.05 ± 0.99	$69.00\pm^{+0.98}_{-0.99}$
$\chi^2_{\rm min}$	13668.898	13671.246	13668.984

Table 5.   Fitting results of the cosmological parameters in the IΛCDM2 $(Q=\beta H\rho_\Lambda)+\sum m_\nu$ model for mass hierarchy cases NH, IH, and DH.

data	Planck TT,TE,EE+lowP+BAO+SNIa+RSD		
model	IΛCDM2+$\sum m_\nu^{\rm NH}$	IΛCDM2+$\sum m_\nu^{\rm IH}$	IΛCDM2+$\sum m_\nu^{\rm DH}$
$\Omega_b h^2$	0.02233 ± 0.00014	0.02235 ± 0.00014	0.02232 ± 0.00014
$\Omega_c h^2$	$0.1319^{+0.0150}_{-0.0068}$	$0.1311^{+0.0153}_{-0.0069}$	$0.1335^{+0.0146}_{-0.0064}$
$100\theta_{\rm MC}$	$1.04017^{+0.00049}_{-0.00083}$	$1.04022^{+0.00049}_{-0.00082}$	$1.04009^{+0.00046}_{-0.00080}$
τ	0.079 ± 0.016	0.082 ± 0.016	$0.074^{+0.017}_{-0.016}$
$\ln(10^{10}A_s)$	3.089 ± 0.032	3.095 ± 0.032	3.080 ± 0.032
n_s	$0.9678^{+0.0040}_{-0.0041}$	0.9685 ± 0.0041	0.9670 ± 0.0042
β	$-0.129^{+0.066}_{-0.146}$	$-0.125^{+0.067}_{-0.151}$	$-0.140^{+0.060}_{-0.141}$
$\sum m_\nu$	<0.206 eV	<0.228 eV	<0.180 eV
$\Omega_{\rm m}$	$0.343^{+0.033}_{-0.018}$	$0.344^{+0.033}_{-0.018}$	$0.343^{+0.032}_{-0.017}$
H_0	$67.32^{+0.54}_{-0.53}$	67.15 ± 0.52	$67.58^{+0.61}_{-0.56}$
$\chi^2_{\rm min}$	13658.662	13659.402	13656.462

favored over the IH case, but the difference $\Delta\chi^2_{\rm min} \equiv \chi^2_{\rm IH;min}-\chi^2_{\rm NH;min} < 2$ (see Tables 5 and 6), which does not seem to be significant enough to distinguish between the mass hierarchies.

3.2   Coupling parameter

In this subsection, we discuss the fitting results of the coupling parameter β. First, we constrain the IΛCDM1+$\sum m_\nu$ model using the Planck TT, TE, EE + lowP + BAO + SNIa + RSD data. The detailed fitting results are given in Table 3. We see that $\beta = 0$ is favored within the 1σ range, regardless of the neutrino mass hierarchy. Furthermore, we constrain the IΛCDM1+$\sum m_\nu$+$N_{\rm eff}$ model using the Planck TT, TE, EE + lowP + BAO + SNIa + RSD + H_0 data. The detailed fitting results are given in Table 4. For this data combination, $\beta = 0$ is still favored by the data.

Thus, there is no evidence of a nonzero interaction in the $Q=\beta H\rho_c$ model. In addition, from Figs. 1 and 2, we see that β is positively correlated with $\sum m_\nu$.

Next, we constrain the IΛCDM2+$\sum m_\nu$ model using the Planck TT, TE, EE + lowP + BAO + SNIa + RSD data, and we constrain the IΛCDM2+$\sum m_\nu$+$N_{\rm eff}$ model using the Planck TT, TE, EE + lowP + BAO + SNIa + RSD + H_0 data. The detailed fitting results are given in Tables 5 and 6, respectively. For the $Q=\beta H\rho_\Lambda$ model, an exciting result is that negative values of β are favored by current observations at more than the 1σ level, indicating that vacuum energy decays into cold dark matter. Further, we see that the values of β are truncated when $\beta<-0.3$. This is because β is anticorrelated with $\Omega_{\rm m}$, as shown in Figs. 3 and 4. A larger $\Omega_{\rm m}$ leads to a smaller β, whereas a too-small value of β (negative value) is not allowed by theory in current cosmology.

Table 6.   Fitting results of the cosmological parameters in the IΛCDM2 ($Q=\beta H\rho_\Lambda$)+$\sum m_\nu$+N_{eff} model for mass hierarchy cases NH, IH, and DH.

data	Planck TT,TE,EE+lowP+BAO+SNIa+RSD+H_0		
model	IΛCDM2+$\sum m_\nu^{\mathrm{NH}}$+N_{eff}	IΛCDM2+$\sum m_\nu^{\mathrm{IH}}$+N_{eff}	IΛCDM2+$\sum m_\nu^{\mathrm{DH}}$+N_{eff}
$\Omega_b h^2$	0.02259 ± 0.00018	0.02264 ± 0.00018	0.02255 ± 0.00018
$\Omega_c h^2$	$0.1415^{+0.0144}_{-0.0076}$	$0.1417^{+0.0144}_{-0.0079}$	$0.1415^{+0.0139}_{-0.0076}$
$100\theta_{\mathrm{MC}}$	$1.03950^{+0.00057}_{-0.00085}$	$1.03947^{+0.00058}_{-0.00084}$	$1.03953^{+0.00056}_{-0.00083}$
τ	0.084 ± 0.017	$0.088^{+0.016}_{-0.017}$	$0.079^{+0.017}_{-0.018}$
$\ln(10^{10}A_s)$	3.109 ± 0.034	3.118 ± 0.033	3.098 ± 0.034
n_s	0.9792 ± 0.0070	0.9811 ± 0.0070	0.9769 ± 0.0071
β	$-0.172^{+0.050}_{-0.122}$	$-0.171^{+0.052}_{-0.122}$	$-0.174^{+0.049}_{-0.118}$
$\sum m_\nu$	<0.215 eV	<0.245 eV	<0.188 eV
N_{eff}	$3.33^{+0.16}_{-0.17}$	3.37 ± 0.17	3.29 ± 0.17
Ω_{m}	$0.344^{+0.028}_{-0.014}$	$0.345^{+0.027}_{-0.014}$	$0.343^{+0.027}_{-0.014}$
H_0	69.30 ± 1.00	69.30 ± 1.00	69.30 ± 1.00
χ^2_{min}	13664.296	13665.398	13664.704
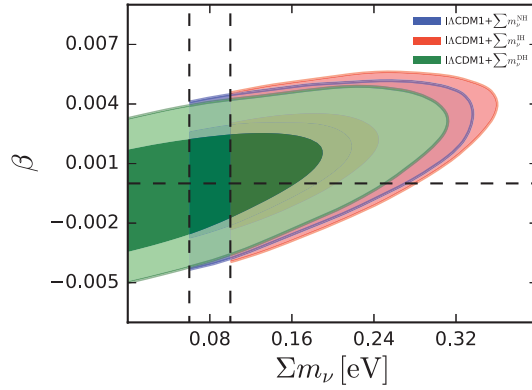
Fig. 1.   (color online) Two-dimensional marginalized contours (1σ and 2σ) of the $\sum m_\nu$–β plane in the IΛCDM1 ($Q=\beta H\rho_{\mathrm{c}}$)+$\sum m_\nu$ model using the Planck TT, TE, EE + lowP + BAO + SNIa + RSD data combination for various neutrino mass hierarchies.
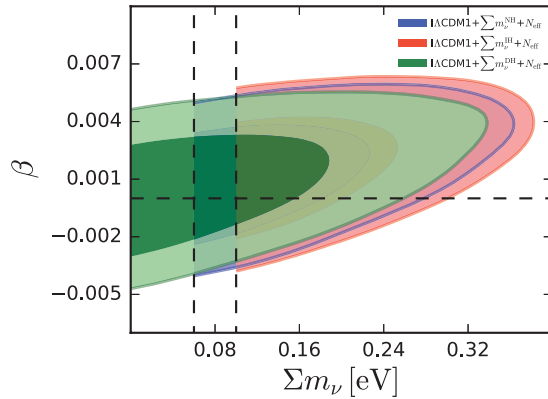
Fig. 2.   (color online) Two-dimensional marginalized contours (1σ and 2σ) of the $\sum m_\nu$–β plane in the IΛCDM1 ($Q=\beta H\rho_{\mathrm{c}}$)+$\sum m_\nu$+$N_{\mathrm{eff}}$ model using the Planck TT, TE, EE + lowP + BAO + SNIa + RSD +H_0 data combination for various neutrino mass hierarchies.
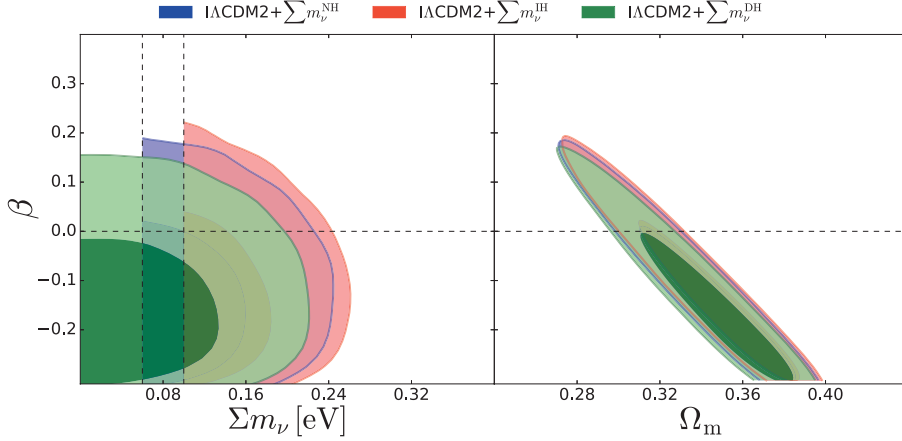
Fig. 3.   (color online) Two-dimensional marginalized contours (1σ and 2σ) of the $\sum m_\nu$–β plane and the Ω_m–β plane in the IΛCDM2 ($Q = \beta H\rho_\Lambda$)+$\sum m_\nu$ model using the Planck TT, TE, EE + lowP + BAO + SNIa + RSD data combination for various neutrino mass hierarchies.
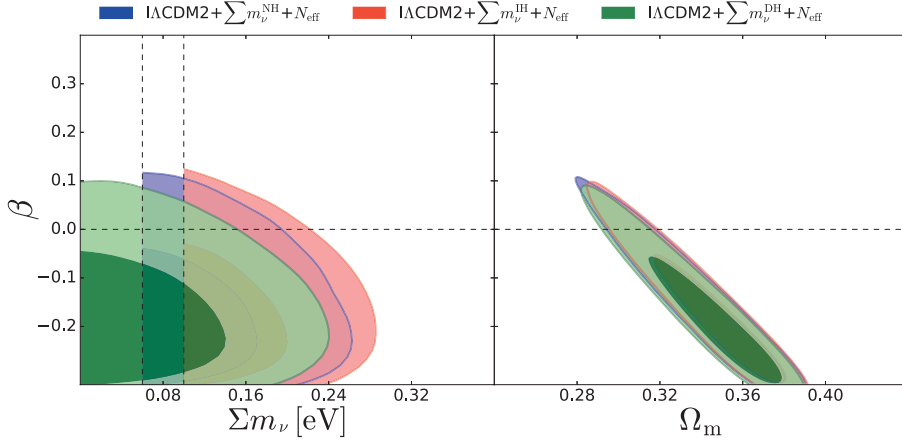

Fig. 4.   (color online) Two-dimensional marginalized contours (1σ and 2σ) of the $\sum m_\nu$–β plane and the Ω_m–β plane in the IΛCDM2 ($Q = \beta H\rho_\Lambda$)+$\sum m_\nu$+N_{eff} model using the Planck TT, TE, EE +lowP +BAO + SNIa + RSD + H_0 data combination for various neutrino mass hierarchies.

4   Conclusion

In this paper, we constrain the total neutrino mass in the scenario of vacuum energy interacting with cold dark matter. We consider three neutrino mass hierarchy cases, i.e., the NH case, the IH case, and the DH case. In our analysis, we employ two data combinations, i.e., the Planck TT, TE, EE + lowP + BAO + SNIa + RSD data combination and the Planck TT, TE, EE + lowP + BAO + SNIa + RSD + H_0 data combination. It is worth mentioning that there is a strong tension between the local measurement of H_0 and the fitting result derived from the Planck data. Thus, when the local measurement of H_0 is used to constrain the models, we consider an additional parameter, N_{eff}, in the cosmological models to relieve the tension.

We find that, compared with the ΛCDM model, the $Q = \beta H\rho_c$ model can provide a much looser constraint on the total neutrino mass, whereas the $Q = \beta H\rho_\Lambda$ model gives a slightly tighter constraint. We also compare the constrained values of $\sum m_\nu$ for the three mass hierarchy cases. We find that the upper limits on $\sum m_\nu$ are smallest in the DH case. By comparing the values of χ^2_{min} for different neutrino mass hierarchies, we find that the NH case is favored over the IH case in the IΛCDM models. The difference $\Delta\chi^2_{\text{min}} \equiv \chi^2_{\text{IH;min}} - \chi^2_{\text{NH;min}}$ is 2.69 in the $Q = \beta H\rho_c$ model. Our results are consistent with those of Refs. [47–49].

In addition, we also probe the interaction between vacuum energy and cold dark matter. For the $Q = \beta H\rho_c$ model, there is no evidence of a nonzero interaction. However, for the $Q = \beta H\rho_\Lambda$ model, we find that a neg-

ative β is favored at more than the 1σ level, indicating that vacuum energy decays into cold dark matter. Our fitting results of the coupling constant β are different from those of Ref. [50]. The reason may be that the lo-

cal H_0 measurement with a strong tension is employed in Ref. [50], whereas in our analysis, we add the parameter $N_{\rm eff}$ to alleviate the tension when the local measurement value of H_0 is employed to constrain the models.

References

1   J. Lesgourgues and S. Pastor, Phys. Rept., **429**: 307 (2006)
2   K. A. Olive et al (Particle Data Group), Chin. Phys. C, **38**: 090001 (2014)
3   A. Osipowicz et al (KATRIN Collaboration), hep-ex/0109033
4   C. Kraus et al, Eur. Phys. J. C, **40**: 447 (2005)
5   E. W. Otten and C. Weinheimer, Rept. Prog. Phys., **71**: 086201 (2008)
6   J. Wolf (KATRIN Collaboration), Nucl. Instrum. Meth. A, **623**: 442 (2010)
7   H. V. Klapdor-Kleingrothaus and U. Sarkar, Mod. Phys. Lett. A, **16**: 2469 (2001)
8   H. V. Klapdor-Kleingrothaus, I. V. Krivosheina, A. Dietz, and O. Chkvorets, Phys. Lett. B, **586**: 198 (2004)
9   S. Betts et al, arXiv:1307.4738 [astro-ph.IM]
10 J. Zhang and S. Zhou, Nucl. Phys. B, **903**: 211 (2016)
11 G. Y. Huang and S. Zhou, Phys. Rev. D, **94**(11): 116009 (2016)
12 J. Zhang and X. Zhang, Nature Commun., **9**: 1833 (2018)
13 M. M. Zhao, Y. H. Li, J. F. Zhang, and X. Zhang, Mon. Not. Roy. Astron. Soc., **469**(2): 1713 (2017)
14 X. Zhang, Phys. Rev. D, **93**(8): 083011 (2016)
15 W. Hu, D. J. Eisenstein, and M. Tegmark, Phys. Rev. Lett., **80**: 5255 (1998)
16 B. A. Reid, L. Verde, R. Jimenez, and O. Mena, JCAP, **1001**: 003 (2010)
17 S. A. Thomas, F. B. Abdalla, and O. Lahav, Phys. Rev. Lett., **105**: 031301 (2010)
18 C. Carbone, L. Verde, Y. Wang, and A. Cimatti, JCAP, **1103**: 030 (2011)
19 H. Li and X. Zhang, Phys. Lett. B, **713**: 160 (2012)
20 Y. H. Li, S. Wang, X. D. Li, and X. Zhang, JCAP, **1302**: 033 (2013)
21 B. Audren, J. Lesgourgues, S. Bird, M. G. Haehnelt, and M. Viel, JCAP, **1301**: 026 (2013)
22 S. Riemer-Sørensen, D. Parkinson, and T. M. Davis, Phys. Rev. D, **89**: 103505 (2014)
23 A. Font-Ribera, P. McDonald, N. Mostek, B. A. Reid, H. J. Seo, and A. Slosar, JCAP, **1405**: 023 (2014)
24 J. F. Zhang, Y. H. Li, and X. Zhang, Phys. Lett. B, **740**: 359 (2015)
25 J. F. Zhang, Y. H. Li, and X. Zhang, Eur. Phys. J. C, **74**: 2954 (2014)
26 J. F. Zhang, J. J. Geng, and X. Zhang, JCAP, **1410**: no. 10, 044 (2014)
27 N. Palanque-Delabrouille et al, JCAP, **1502**(2): 045 (2015)
28 C. Q. Geng, C. C. Lee, and J. L. Shen, Phys. Lett. B, **740**: 285 (2015)
29 Y. H. Li, J. F. Zhang, and X. Zhang, Phys. Lett. B, **744**: 213 (2015)
30 P. A. R. Ade et al (Planck Collaboration), Astron. Astrophys., **594**: A13 (2016)
31 J. F. Zhang, M. M. Zhao, Y. H. Li, and X. Zhang, JCAP, **1504**: 038 (2015)
32 C. Q. Geng, C. C. Lee, R. Myrzakulov, M. Sami, and E. N. Saridakis, JCAP, **1601**(01): 049 (2016)
33 Y. Chen and L. Xu, Phys. Lett. B, **752**: 66 (2016)
34 R. Allison, P. Caucal, E. Calabrese, J. Dunkley, and T. Louis, Phys. Rev. D, **92**: no. 12, 123535 (2015)
35 A. J. Cuesta, V. Niro, and L. Verde, Phys. Dark Univ., **13**: 77 (2016)
36 Y. Chen, B. Ratra, M. Biesiada, S. Li, and Z. H. Zhu, Astrophys. J., **829**(2): 61 (2016)
37 M. Moresco, R. Jimenez, L. Verde, A. Cimatti, L. Pozzetti, C. Maraston, and D. Thomas, JCAP, **1612**(12): 039 (2016)
38 J. Lu, M. Liu, Y. Wu, Y. Wang, and W. Yang, Eur. Phys. J. C, **76**(12): 679 (2016)
39 S. Kumar and R. C. Nunes, Phys. Rev. D, **94**(12): 123511 (2016)
40 L. Xu and Q. G. Huang, Sci. China Phys. Mech. Astron., **61**(3): 039521 (2018)
41 S. Vagnozzi, E. Giusarma, O. Mena, K. Freese, M. Gerbino, S. Ho, and M. Lattanzi, Phys. Rev. D, **96**(12): 123503 (2017)
42 X. Zhang, Sci. China Phys. Mech. Astron., **60**(6): 060431 (2017)
43 C. S. Lorenz, E. Calabrese, and D. Alonso, Phys. Rev. D, **96**(4): 043510 (2017)
44 M. M. Zhao, J. F. Zhang, and X. Zhang, Phys. Lett. B, **779**: 473 (2018)
45 S. Vagnozzi, S. Dhawan, M. Gerbino, K. Freese, A. Goobar, and O. Mena, arXiv:1801.08553 [astro-ph.CO]
46 L. F. Wang, X. N. Zhang, J. F. Zhang, and X. Zhang, Phys. Lett. B, **782**: 87 (2018)
47 Q. G. Huang, K. Wang, and S. Wang, Eur. Phys. J. C, **76**(9): 489 (2016)
48 S. Wang, Y. F. Wang, D. M. Xia, and X. Zhang, Phys. Rev. D, **94**(8): 083519 (2016)
49 W. Yang, R. C. Nunes, S. Pan, and D. F. Mota, Phys. Rev. D, **95**(10): 103522 (2017)
50 R. Y. Guo, Y. H. Li, J. F. Zhang, and X. Zhang, JCAP, **1705**(05): 040 (2017)
51 L. Amendola, Phys. Rev. D, **62**: 043511 (2000)
52 L. Amendola and D. Tocchini-Valentini, Phys. Rev. D, **66**: 043528 (2002)
53 D. Comelli, M. Pietroni, and A. Riotto, Phys. Lett. B, **571**: 115 (2003)
54 R. G. Cai and A. Wang, JCAP, **0503**: 002 (2005)
55 X. Zhang, Mod. Phys. Lett. A, **20**: 2575 (2005)
56 W. Zimdahl, Int. J. Mod. Phys. D, **14**: 2319 (2005)
57 X. Zhang, F. Q. Wu, and J. Zhang, JCAP, **0601**: 003 (2006)
58 B. Wang, J. Zang, C. Y. Lin, E. Abdalla, and S. Micheletti, Nucl. Phys. B, **778**: 69 (2007)
59 Z. K. Guo, N. Ohta, and S. Tsujikawa, Phys. Rev. D, **76**: 023508 (2007)
60 O. Bertolami, F. Gil Pedro, and M. Le Delliou, Phys. Lett. B, **654**: 165 (2007)
61 J. Zhang, H. Liu, and X. Zhang, Phys. Lett. B, **659**: 26 (2008)
62 C. G. Boehmer, G. Caldera-Cabral, R. Lazkoz, and R. Maartens, Phys. Rev. D, **78**: 023505 (2008)
63 J. Valiviita, E. Majerotto, and R. Maartens, JCAP, **0807**: 020 (2008)
64 J. H. He and B. Wang, JCAP, **0806**: 010 (2008)
65 J. H. He, B. Wang, and Y. P. Jing, JCAP, **0907**: 030 (2009)
66 J. H. He, B. Wang, and P. Zhang, Phys. Rev. D, **80**: 063530 (2009)
67 K. Koyama, R. Maartens, and Y. S. Song, JCAP, **0910**: 017 (2009)
68 J. Q. Xia, Phys. Rev. D, **80**: 103514 (2009)
69 M. Li, X. D. Li, S. Wang, Y. Wang, and X. Zhang, JCAP,

0912: 014 (2009)

70 L. Zhang, J. Cui, J. Zhang, and X. Zhang, Int. J. Mod. Phys. D, **19**: 21 (2010)

71 H. Wei, Commun. Theor. Phys., **56**: 972 (2011)

72 Y. Li, J. Ma, J. Cui, Z. Wang, and X. Zhang, Sci. China Phys. Mech. Astron., **54**: 1367 (2011)

73 J. H. He, B. Wang, and E. Abdalla, Phys. Rev. D, **83**: 063515 (2011)

74 Y. H. Li and X. Zhang, Eur. Phys. J. C, **71**: 1700 (2011)

75 T. F. Fu, J. F. Zhang, J. Q. Chen, and X. Zhang, Eur. Phys. J. C, **72**: 1932 (2012)

76 Z. Zhang, S. Li, X. D. Li, X. Zhang, and M. Li, JCAP, **1206**: 009 (2012)

77 J. Zhang, L. Zhao, and X. Zhang, Sci. China Phys. Mech. Astron., **57**: 387 (2014)

78 Y. H. Li and X. Zhang, Phys. Rev. D, **89**(8): 083009 (2014)

79 J. J. Geng, Y. H. Li, J. F. Zhang, and X. Zhang, Eur. Phys. J. C, **75**(8): 356 (2015)

80 J. L. Cui, L. Yin, L. F. Wang, Y. H. Li, and X. Zhang, JCAP, **1509**(09): 024 (2015)

81 R. Murgia, S. Gariazzo, and N. Fornengo, JCAP, **1604**: no. 04, 014 (2016)

82 J. Solà, A. Gómez-Valent, and J. de Cruz Pérez, Astrophys. J., **836**(1): 43 (2017)

83 B. Wang, E. Abdalla, F. Atrio-Barandela, and D. Pavon, Rept. Prog. Phys., **79**(9): 096901 (2016)

84 A. Pourtsidou and T. Tram, Phys. Rev. D, **94**(4): 043518 (2016)

85 A. A. Costa, X. D. Xu, B. Wang, and E. Abdalla, JCAP, **1701**(01): 028 (2017)

86 J. Sola, J. de Cruz Pérez, A. Gomez-Valent, and R. C. Nunes, arXiv:1606.00450 [gr-qc]

87 L. Feng and X. Zhang, JCAP, **1608**(08): 072 (2016)

88 D. M. Xia and S. Wang, Mon. Not. Roy. Astron. Soc., **463**: 952 (2016)

89 C. van de Bruck, J. Mifsud, and J. Morrice, Phys. Rev. D, **95**(4): 043513 (2017)

90 J. Sola, Int. J. Mod. Phys. A, **31**(23): 1630035 (2016)

91 S. Kumar and R. C. Nunes, Phys. Rev. D, **96**(10): 103511 (2017)

92 J. Sola, J. d. C. Perez, and A. Gomez-Valent, arXiv:1703.08218 [astro-ph.CO]

93 V. Salvatelli, N. Said, M. Bruni, A. Melchiorri, and D. Wands, Phys. Rev. Lett., **113**(18): 181301 (2014)

94 L. Feng, J. F. Zhang, and X. Zhang, arXiv:1712.03148 [astro-ph.CO]

95 A. J. Ross, L. Samushia, C. Howlett, W. J. Percival, A. Burden and M. Manera, Mon. Not. Roy. Astron. Soc., **449**(1): 835 (2015)

96 F. Beutler et al, Mon. Not. Roy. Astron. Soc., **416**: 3017 (2011)

97 L. Anderson et al (BOSS Collaboration), Mon. Not. Roy. Astron. Soc., **441**(1): 24 (2014)

98 M. Betoule et al (SDSS Collaboration), Astron. Astrophys., **568**: A22 (2014)

99 A. G. Riess et al, Astrophys. J., **826**(1): 56 (2016)

100 H. Gil-Marín, W. J. Percival, L. Verde, J. R. Brownstein, C. H. Chuang, F. S. Kitaura, S. A. Rodríguez-Torres, and M. D. Olmstead, Mon. Not. Roy. Astron. Soc., **465**(2): 1757 (2017)

101 E. Di Valentino and F. R. Bouchet, JCAP, **1610**(10): 011 (2016)

102 X. Zhang, Sci. China Phys. Mech. Astron., **60**(6): 060421 (2017)

103 M. Benetti, L. L. Graef, and J. S. Alcaniz, JCAP, **1704**(04): 003 (2017)

104 R. Y. Guo and X. Zhang, Eur. Phys. J. C, **77**(12): 882 (2017)

105 R. Y. Guo, L. Zhang, J. F. Zhang, and X. Zhang, arXiv:1801.02187 [astro-ph.CO]

106 P. A. R. Ade et al (Planck Collaboration), Astron. Astrophys., **594**: A14 (2016)

107 Y. H. Li, J. F. Zhang, and X. Zhang, Phys. Rev. D, **90**(6): 063005 (2014)

108 Y. H. Li, J. F. Zhang, and X. Zhang, Phys. Rev. D, **90**(12): 123007 (2014)

109 Y. H. Li, J. F. Zhang, and X. Zhang, Phys. Rev. D, **93**(2): 023002 (2016)

110 X. Zhang, Sci. China Phys. Mech. Astron., **60**(5): 050431 (2017)

111 A. Lewis and S. Bridle, Phys. Rev. D, **66**: 103511 (2002)